

[Invited Paper]

# The Development of gearless reducers with rolling balls<sup>†</sup>

Hidetsugu Terada<sup>\*</sup>

Graduate school of Medical and Engineering, Department of Mechanical System Engineering,  
University of Yamanashi, Takeda 4-3-11, Kofu, Yamanashi 400-8511, Japan

(Manuscript Received May 1, 2009; Revised November 10, 2009; Accepted November 16, 2009)

## Abstract

To satisfy the various demands such as no-backlash characteristic and so on, we have newly developed three types of no-backlash reducers: the cycloid ball reducer, the precession ball reducer and the reciprocating motion input type ball reducer. Especially, these reducers are developed for the robot joints. Also, these reducers are a kind of the constant velocity cam mechanisms with rolling balls; their inputs use eccentric motion, precession motion and reciprocating motion. The motion principle and the profile calculation method of each reducer are proposed, using the vector analysis.

*Keywords:* Ball reducer; No-backlash; Eccentric motion; Precession motion; Reciprocating motion

## 1. Introduction

The characteristic of a no-backlash transmission is the most important performance for industrial robots. To satisfy that performance, many varieties of the no-backlash reducers have been developed [1-3]. However, the conventional no-backlash reducers have a limited reduction ratio. So, we cannot select an arbitrary reduction ratio. Also, these reducers cannot often be used to the robot wrist joint; that size is limited strictly. And the conventional orthogonal axis output type reducers cannot eliminate the backlash. To solve these problems, it is difficult to develop only one type of reducer. Therefore, we have paid attention as follows:

- (1) The planetary motion can generate the reduced rotation with high reduction ratio.
- (2) The cam mechanism is designed using motion loci; that is, no-backlash in theoretical calculation.
- (3) The simplest rolling element is the ball shape.

Considering these points, we have developed three input motion type reducers which are a kind of the constant velocity cam mechanisms with rolling balls; they have eccentric motion, precession motion and reciprocating motion. The eccentric input type is useful for the co-axial output type reducer. And the precession motion input type is useful to generate the reduced orthogonal axis output rotation. Also, the reciprocating motion input type is suitable for the hollow shape and the large diameter of the reducer elements.

<sup>†</sup> This paper was presented at the ICMDT 2009, Jeju, Korea, June 2009. This paper was recommended for publication in revised form by Guest Editors Sung-Lim Ko, Keiichi Watanuki.

<sup>\*</sup>Corresponding author. Tel.: +81 55 220 8452, Fax.: +81 55 220 8452

E-mail address: terada@yamanashi.ac.jp

© KSME & Springer 2010

In this report, an overview of the developed reducers is shown. And the motion principle and the profile calculation method are shown, using the some developed reducers.

## 2. Development of the eccentric motion input type ball reducer

### 2.1 Single stage type cycloid ball reducer

The single stage type cycloid ball reducer [4] consists of two sections: the reduction section and the motion transmitting section with many circular grooves, shown in Fig. 1. The reduction section is driven by the eccentric input shaft shown in Fig. 1 as 1. To eliminate the excitation which is caused by eccentric motion, a counter weight is needed as 2. The reduction section consists of a fixed disc 4 with an epi-trochoidal

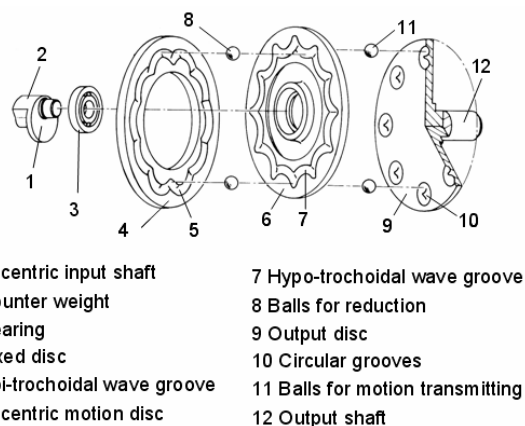


Fig. 1. Fundamental structure of a single stage type cycloid ball reducer.

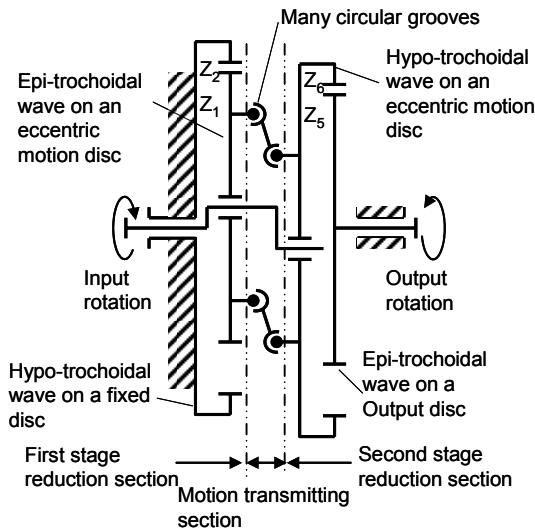


Fig. 2. Equivalent model of a two stage type cycloid ball reducer.

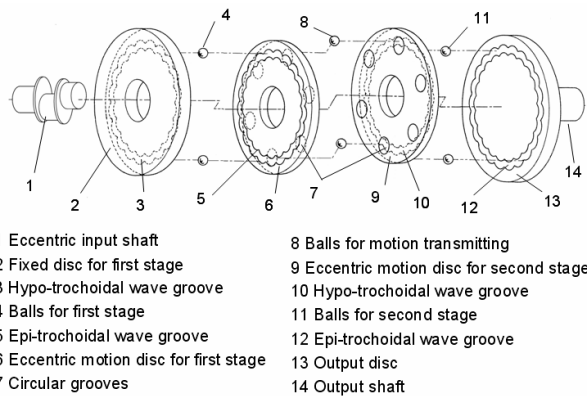


Fig. 3. Fundamental structure of a two stage type cycloid ball reducer.

wave groove 5, an eccentric motion disc 6 with a hypo-trochoidal wave groove 7, and many rolling balls 8. To eliminate the eccentric rotation, the motion transmitting section consists of many rolling balls 11, the circular grooves 10 of the eccentric motion disc 8 which are arranged on the opposite side of a trochoidal wave groove, and the output disc 9 with circular grooves. Also, the generated reduced motion rotates the output shaft 12.

**2.2 Two stage type cycloid ball reducer**

At the single stage type reducer, to eliminate the excitation which is caused by eccentric motion, a counterweight is needed. Furthermore, the improvement of reducer configuration is necessary to satisfy the light weight and small size. So, we have developed a two-stage type cycloid ball reducer [5] that consists of two sections, the reduction section and the motion transmitting section with many circular grooves, shown in Fig. 2. Each fundamental element is similar to the single stage type reducer, as shown in Fig. 3. Each terminology is defined in Table 1.

Table 1. Terminology of a two stage type trochoidal wave ball reducer.

Symbol	Terminology
$r_{0a}$	Standard radius of a trochoid curve at first stage
$r_{0b}$	Standard radius of a trochoid curve at second stage
$\alpha_a$	Trochoid factor of a trochoid curve at first stage
$\alpha_b$	Trochoid factor of a trochoid curve at second stage
$\delta$	First stage reduced rotation angle
$\tau$	Second stage reduced rotation angle
$\theta_{in}$	Input rotation angle
$n_1$	Number of the first stage epi-trochoidal wave groove
$n_2$	Number of the first stage hypo-trochoidal wave
$n_5$	Number of the second stage epi-trochoidal wave
$n_6$	Number of the second stage hypo-trochoidal wave

**2.3 Kinematic analysis of a reduction section**

In general, the epi/hypo-trochoidal curve is well known as the locus of the arbitrary point on the rolling circle without slipping around the base circle. To decide the arbitrary position on the rolling circle, we have newly defined the trochoid factor. So, using the standard radius, the trochoid factor and the number of trochoidal wave on each base circle, epi-trochoidal curve  $P_3$  is defined as Eq. (1) and the hypo-trochoidal curve  $P_4$  is defined as Eq. (2).

$$P_3 = (n_1 + 1)r_{0a}e^{j\theta_3} - \alpha_a \cdot r_{0a}e^{j(1+n_1)\theta_3} \tag{1}$$

$$P_4 = (n_2 - 1)r_{0a}e^{j\theta_4} + \alpha_a \cdot r_{0a}e^{j(1-n_2)\theta_4} \tag{2}$$

The trochoid factor  $\alpha_a$  defines the shape of the trochoidal curve. In cases in which that factor is 1.0, that curve has a cycloidal shape, and when that is higher than 1.0, that curve has a wave shape with a loop. Therefore, the trochoid factor should be selected as Eq. (3).

$$0 < \alpha_a \leq 1.0 \tag{3}$$

And the eccentricity  $e_1$  is defined as shown in Eq. (4).

$$e_1 = 2\alpha_a \cdot r_{0a} \tag{4}$$

The center locus of the wave groove on each disc conforms to the trochoidal curve, so we analyze the center loci. And when the fixed disc has a hypo-trochoidal wave groove, and the eccentric motion disc has an epi-trochoidal wave groove, the geometry of a reduction section is shown in Fig. 4. The motion of the epi-trochoidal wave locus  $P_2$  on the eccentric motion disc is defined by Eq. (5).

$$P_2 = 2\alpha_a \cdot r_{0a}e^{j\theta_m} + e^{j\delta} \cdot P_3 \\ = 2\alpha_a \cdot r_{0a}e^{j\theta_m} \\ + (n_1 + 1)r_{0a}e^{j(\theta_3+\delta)} - \alpha_a \cdot r_{0a}e^{j(1+n_1)\theta_3+\delta} \tag{5}$$

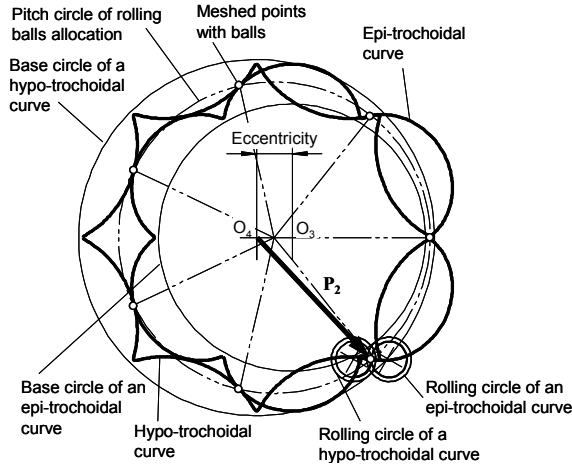


Fig. 4. Geometry of an epi-trochoidal wave and a hypo-trochoidal wave meshing.

In this equation, the  $\delta$  shows the reduced rotation angle around the first stage eccentric shaft. On the other hand, the hypo-trochoidal wave groove on the fixed disc conforms to Eq. (2). When these grooves are meshed across many balls, as shown in Fig. 4, the first stage design conditions are needed as follows.

$$\begin{cases} n_2 - n_1 = 2 \\ \delta = -\frac{2}{n_1} \theta_{in} \\ \theta_3 = \frac{n_1 + 2}{n_1(n_1 + 1)} \theta_{in} \\ \theta_4 = \frac{-1}{n_1 + 1} \theta_{in} \end{cases} \quad (6)$$

The motion of the epi-trochoidal wave locus  $P_2$  is shown in Eq. (7). This equation is satisfied on the arbitrary rotation.

$$P_2 = (n_1 + 1)r_{0a} e^{j\left\{\frac{1}{n_1+1}(\theta_{in} + 2m\pi)\right\}} + \alpha_a \cdot r_{0a} e^{j\theta_{in}} \quad (m = 0, 1, 2, \dots, n_1) \quad (7)$$

In cases in which all meshed points with balls conform to the points on tangents of the epi-trochoidal curve and the hypo-trochoidal curve, all balls are arranged to the equivalent pitch. The number of balls is  $n_1 + 1$ .

At the second stage section, the motion analysis is similar to the first stage section. However, to rotate with a constant velocity, the  $f_1$  must be an integer which shows the design condition parameter of wave numbers, as Eq. (8).

$$f_1 = \frac{n_1 + 2 \cdot (n_5 + 2)}{n_1} \quad (8)$$

So the relation between the number of a first stage epi-trochoidal wave  $n_5$  and the reduction ratio  $i$  is needed as shown in Fig. 5.

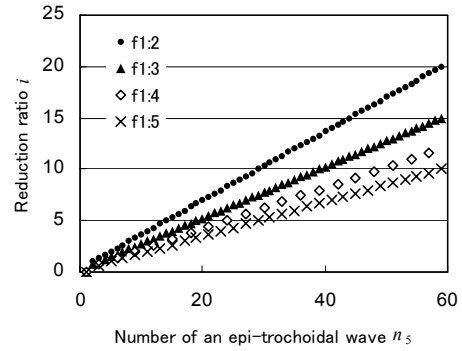


Fig. 5. Relation between the numbers of a stage epi-trochoidal wave.

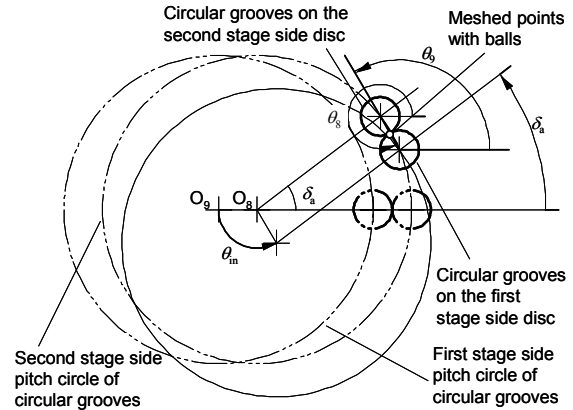


Fig. 6. Geometry of a circular groove wave meshing.

#### 2.4 Kinematic analysis of a motion transmitting section

At the two stage type reducer, the two reduction sections are driven by two eccentricities which are not equal. So, the transmitting section is needed to eliminate the different rotational phase and the different eccentricities. The circular grooves of the eccentric motion discs are arranged on the opposite side of each trochoidal wave groove. The geometrical model is shown in Fig. 6. The eccentricity of the second stage  $e_2$  is defined as shown in Eq. (9).

$$e_2 = 2\alpha_b \cdot r_{0b} \quad (9)$$

The second stage eccentricity is arranged on an opposite phase to each other. The initial position of circular grooves is located on an opposite phase, too. Using Eq. (7), the standard radius  $r_8$ , the circular groove radius  $r_7$ , and rotation angle of each stage  $\theta_8, \theta_7$ , the circular locus curve  $P_8$  on the first stage side are defined as Eq. (10), and the circular locus curve  $P_7$  on the second stage side is defined as Eq. (11).

$$P_8 = 2\alpha_a \cdot r_{0a} e^{j\theta_{in}} + r_8 e^{j\delta} + (\alpha_a \cdot r_{0a} + \alpha_b \cdot r_{0b}) e^{j\theta_b} \quad (10)$$

$$P_7 = -2\alpha_b \cdot r_{0b} e^{j\theta_{in}} + r_7 e^{j\gamma} + (\alpha_a \cdot r_{0a} + \alpha_b \cdot r_{0b}) e^{j\theta_7} \quad (11)$$

In this equation, the  $\gamma$  shows the reduced rotation angle around the second stage eccentric shaft. When these grooves are

meshed across many balls, the design conditions are needed as Eq. (12).

$$\begin{cases} r_8 = r_7 \\ \delta = \gamma = -\frac{2}{n_2} \theta_{in} \\ \theta_7 = \theta_{in} \\ \theta_8 = \theta_{in} + \pi \end{cases} \quad (12)$$

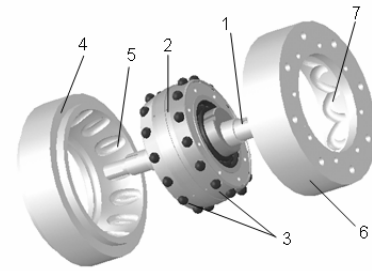
### 3. Development of the precession motion input type ball reducer

#### 3.1 Co-axial output type precession ball reducer

The co-axial type precession ball reducer [6] consists of an inclined input shaft 1, a precession motion rotor 2 which rotates around the input shaft freely, many rolling balls on the rotor 3, a fixed ring 4 with spatial circular grooves 5 of an inside surface and an output ring 6 with the trochoidal wave groove 7 of an inside surface, as shown Fig. 7. The output ring has a coaxial output to the input shaft. Many balls which are arranged on the rotor are meshing with the spatial circular grooves 5, to generate a precession motion of pre-cession rotor. The spatial cycloidal or trochoidal wave groove 7, which is based on a precession motion, generates the reduced rotating motion. That spatial wave groove is the locus of a precession motion with the reduced rotating motion, which generates using the relative motion of a precession rotor and an output ring. On both sides of the pre-cession rotor, many rotating balls are arranged in a uniform angular pitch. For each ball, the rotating phase which is caused by an inclined input shaft is different.

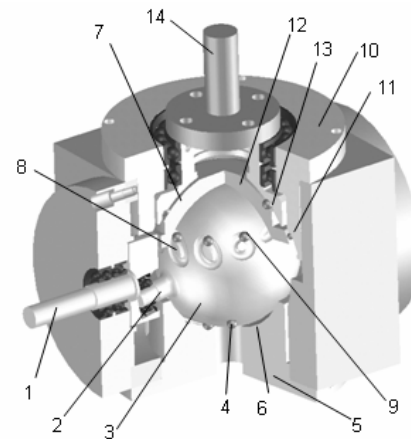
#### 3.2 Orthogonal-axis output type precession ball reducer

The orthogonal-axis output type precession ball reducer [7] consists of many parts as shown in Fig. 8. The generating section of precession motion consists of an inclined input shaft 1 with the inclined shaft 2 which rotates freely, a precession motion rotor 3 which rotates around the input shaft freely, many rolling balls 4 for precession motion and a fixed ring 5 with the spatial circular grooves 6 of an inside surface. These spatial circular grooves make the precession motion. The converting section of the precession motion direction consists of a converting rotor 7 and many rolling balls 9, 11 and 13 on that rotor. The precession rotor has many grooves 8 for converting that motion direction. And many circular grooves 10 are assigned around that rotor, to generate precession motion around the output axis. Also, the section of reduced output motion consists of an output rotor with the spatial trochoidal-wave groove 12 of an inside surface. This groove is generated from the arbitrary required reduction ratio. The generated reduced motion rotates the output shaft 14 which is the orthogonal direction of the input shaft.



1 Inclined input shaft  
2 Precession motion rotor  
3 Balls  
4 Fixed ring  
5 Circular grooves  
6 Output ring  
7 Trochoidal wave groove

Fig. 7. Fundamental structure of a co-axial type precession ball reducer.



1 Input shaft  
2 Inclined shaft  
3 Precession motion rotor  
4 Balls for precession motion  
5 Fixed ring  
6 Grooves for precession motion  
7 Converting rotor of precession motion  
8 Grooves for motion converting  
9 Balls for motion converting  
10 Fixed ring for orthogonal precession motion with circular grooves  
11 Balls for orthogonal precession motion  
12 Reduced ring with wave groove  
13 Balls for reduced motion  
14 Output shaft

Fig. 8. Fundamental structure of an orthogonal axial type precession ball reducer.

#### 3.3 Kinematic analysis of spatial circular grooves on the fixed ring

In general, the precession motion is well known as the rotating motion of a cone without slipping. This motion can be modeled to the motion of a disc rotating around the equivalent circle in which the rotating axis coincides with the *i*-axis on the Cartesian space. When a precession motion is generated, it is necessary to limit the arbitrary spatial motion. So, spatial circular grooves on fixed ring are needed. Also, the reduced rotating motion is generated from the precession motion for the precession rotor. The reaction torque for reduced rotating motion acts on the precession rotor. So the mechanism which holds a reaction torque is needed as well as the general planetary gearing system, at this proposed reducer. Therefore, the circular spatial grooves on a fixed ring are investigated.

The section generating the precession motion is shown in Fig. 9. The axis of the input shaft intersects with the inclined shaft at the origin point  $O_p$ . Then the pitch radius of balls located is defined as  $r_0$ . All balls are located on the arbitrary position on a precession rotor, so the number of located balls is defined as  $n$ . Each ball is located around the rotating axis  $w_1$  at the initial angle  $\lambda_n$ . That is separated at the initial angle  $\tau_n$  around  $j$ -axis. Also the inclined angle is defined as  $\alpha_1$  that rotor which rotates freely is assembled to the inclined shaft.

When the inclined input shaft rotates as  $\theta$ , the precession rotor rotates without slipping on the equivalent disc as  $\phi_1$ . So the position of the ball center  $\mathbf{P}_1$  is defined as Eq. (13) [13].

$$\mathbf{P}_1 = \mathbf{E}^{w_1\phi_1} \mathbf{E}^{i\theta} \cdot \mathbf{E}^{w_1\lambda_n} \mathbf{E}^{j\tau_n} \mathbf{E}^{j\tau_n} \mathbf{R}_0 = \mathbf{E}^{w_1\phi_1} \mathbf{E}^{j\theta} \cdot \mathbf{P}_0$$

$$n = (0, 1, 2, \dots, Z_{bn} - 1) \tag{13}$$

In this equation, each ball is numbered as the  $n$ -th. Also, the initial position is defined as Eq. (14).

$$\mathbf{R}_0 = (0, 0, -r_0)^T \tag{14}$$

The rotating matrix around the  $w_1$  axis is defined as Eq. (15).

$$\mathbf{E}^{w_1\phi_1} = \begin{bmatrix} \cos\phi_1 + \lambda^2(1 - \cos\phi_1) & & & \\ \lambda\mu(1 - \cos\phi_1) + \nu\sin\phi_1 & & & \\ \nu\lambda(1 - \cos\phi_1) - \mu\sin\phi_1 & & & \\ \lambda\mu(1 - \cos\phi_1) - \nu\sin\phi_1 & \nu\lambda(1 - \cos\phi_1) + \mu\sin\phi_1 & & \\ \cos\phi_1 + \mu^2(1 - \cos\phi_1) & \mu\nu(1 - \cos\phi_1) - \lambda\sin\phi_1 & & \\ \mu\nu(1 - \cos\phi_1) + \lambda\sin\phi_1 & \cos\phi_1 + \nu^2(1 - \cos\phi_1) & & \end{bmatrix} \tag{15}$$

At this equation, the  $\lambda$ ,  $\mu$  and  $\nu$  are defined as the directional cosine of a unit vector at the  $w_1$ -axis.

Based on these vector analyses, the end-mill cutter generates circular grooves the diameter of which is the same as the ball. When these grooves are generated, that cutter pose has to conform to the direction of  $\mathbf{P}_1$ .

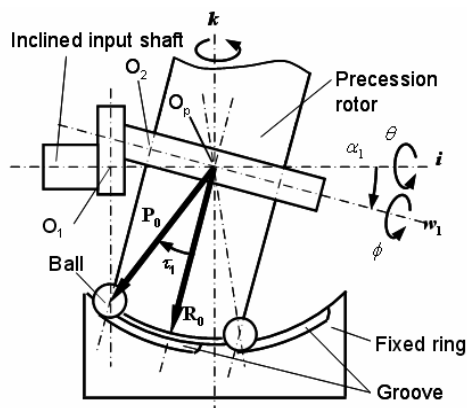


Fig. 9. Geometry of a precession motion and circular groove vector.

### 3.4 Kinematic analysis of the special circular grooves on a converting rotor

The precession motion generated from an input rotating is shown as Eq. (13). However, the axis of output rotating is located on orthogonal direction to the axis of input rotating. So, it is different from the required precession motion which rotates around output axis as shown Eq. (16).

$$\mathbf{P}'_1 = \mathbf{E}^{w_2\phi_2} \mathbf{E}^{k\theta} \mathbf{P}'_0 \tag{16}$$

Each ball on the converting rotor rotates around axis  $w_2$ . That is separated at the initial angle  $\tau_1$  around  $j$ -axis. Also the inclined angle of output side is defined as  $\alpha_2$ . The pitch radius of balls on the converting rotor is defined as Eq. (17).

$$\mathbf{R}'_0 = (r_0, 0, 0)^T \tag{17}$$

The position of each ball is defined as Eq. (18).

$$\mathbf{P}'_0 = \mathbf{E}^{k\epsilon} \mathbf{E}^{w_2\lambda_n} \mathbf{E}^{j\alpha_2} \mathbf{E}^{j\tau_1} \mathbf{R}'_0$$

$$n = (0, 1, 2, \dots, Z_{bn} - 1) \tag{18}$$

In this equation, each ball is numbered as the  $n$ -th. Also, the arbitrary initial pose of a converting rotor is defined as the offset angle  $\epsilon$ .

In cases in which motion is converted on the co-ordinate frame of that rotor, the grooves on the converting rotor are generated with consideration of the relative motion. So, the position of the ball center is calculated, which is similar to the spatial circular grooves on the fixed ring. The example of the special circular shape loci and grooves is shown in Fig. 10. These loci have the individual non-symmetrical circular shapes.

### 3.5 Kinematic analysis of the spatial trochoidal wave groove on an output rotor

The input rotation at 360 degrees generates one cycle of precession motion for that precession rotor around the  $i$ -axis. This motion is limited using the spatial circular grooves on a fixed ring. Then, this motion is converted to the precession motion around the  $k$ -axis using the converting rotor. Also, the reduced rotating motion is generated from the converting rotor

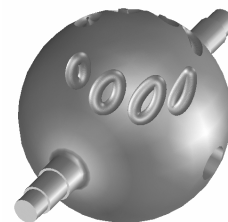


Fig. 10. Special circular shape grooves on the precession motion converting rotor.

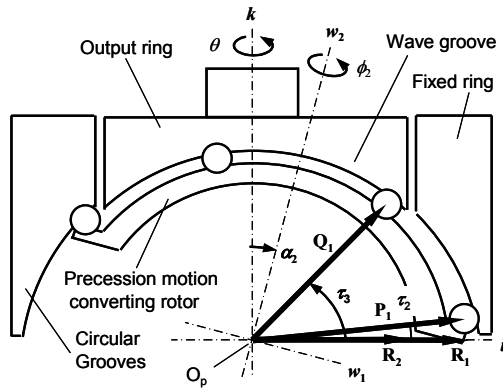


Fig. 11. Geometry of a reduced output motion.

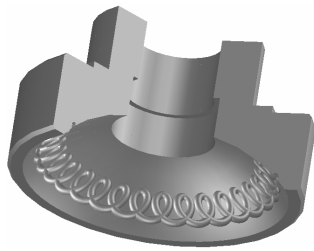


Fig. 12. Trochoidal wave groove on an output ring.

motion. The reaction torque of reduced rotating motion around the  $k$ -axis acts on that converting rotor. So, this section consists of the part which limits spatial motion around the  $k$ -axis, and the generating part of a reduced motion. This generating section of reduced output motion is shown in Fig. 11. The spatial trochoidal wave groove is shown in Fig. 12. With this type of reducer, the rolling balls are arranged in a uniform angular pitch on the rotor converting the precession motion. Therefore, each ball does not separate from that locus at these loop points and rotates smoothly. In other words, the loops on the trochoidal wave groove can be used.

#### 4. Development of the precession motion input type ball reducer

The reciprocating motion type ball reducer [8] consists of the reciprocating motion generating section and the reduced motion generating section. Each element is an input rotor 1, a fixed rotor 2, a reduced motion rotor 3, many reciprocating motion sliders 4 and many rolling balls 5 and 6, as shown in Fig. 13. These sliders are located between the fixed rotor and each input/reduced rotor to hold the rolling balls. Each rotor meshes with balls by use of the outside groove on themselves. Also, the fixed rotor has internal linear grooves 7, which generate the reciprocating motion by ball rolling.

At the reciprocating motion generating section, to generate the doubling reciprocating cycle motion using the constant velocity input rotation, the input rotor has a special circulate groove 8, just like a "8" character, which is on the rotor outside surface. The meshing with the ball located on that slider and the groove generates the half speed reciprocating motion.

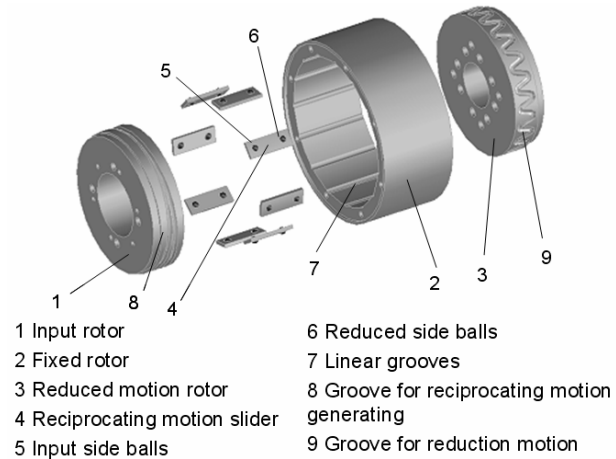


Fig. 13. Structure of a reciprocating motion ball reducer.

That ball meshes with fixed rotor simultaneously. The motion direction is translated by use of the component of the reciprocating motion direction. It is similar to a grooved cam mechanism which has a converting follower. Also, at this section, many reciprocating motion sliders which have different motion phase each other are assigned on the uniform angular pitch.

On the other hand, at the reduced motion generating section, the reduced rotation is generated by use of the meshing with balls and the reduced groove. These balls are located on the reciprocating motion slider. That groove has a wave groove just like a "trochoidal-wave" 9 on that rotor outside surface. At this section, these reciprocating sliders drive a reduced motion rotor which is different from the general cam mechanism.

#### 5. Conclusions

In this report, an overview of reducers which were developed to satisfy the various demands is given. Using the two stage type cycloid ball reducer and the orthogonal-axis output type precession ball reducer, the motion principle and the profile calculation method are shown.

In future work, to realize higher performances for the robot joint, we'll improve the structures of reducers.

#### References

- [1] W. G. Molyneux, The follower tooth reduction gear, *Mechanisms 1972*, I. Mech. E., London, G.B., (1973) 15-23.
- [2] *Cyclo Reducer catalog*, Sumitomo Heavy Industry Ltd., Tokyo, Japan, (1999) F0101-2.
- [3] *Harmonic Drive CSF-3 Series Technical Data*, Harmonic Drive systems Inc., Tokyo, Japan, (2008) 0710-2R-TCSF3.
- [4] H. Terada, K. Imase and H. Makino, Fundamental analysis of a cycloid ball reducer, (1st report) Motion principle, *J. Japan Soc. for Precision Engineering* 54(11) (1988) 2101-2106.
- [5] H. Terada and K. Imase, Motion analysis of a multi-stage type trochoidal wave ball reducer, *Proc. of the 10th Int. Conf.*

on the Theory of Machines and Mechanisms, Liberec, Czech Republic, (2008) 629-636.

- [6] H. Terada, T. Fukazawa and R. Irie, Motion analysis of a coaxial output type precession motion ball reducer, *Proc. of the 11th World Congress in Mechanism and Machine Science*, Tianjin, China, (2004) 877-881.
- [7] H. Terada and R. Irie, Motion analysis of an orthogonal output type precession motion ball reducer, *Proc. of the 9th Int. Conf. on the Theory of Machines and Mechanisms*, Liberec, Czech Republic, (2004) 753-762.
- [8] H. Terada, T. Masuda and S. Yoshida, Motion analysis of a reciprocating motion type ball reducer, *Proc. of the 12th World Congress in Mechanism and Machine Science*, Besancon, France, (2007) Lc4-418.



**Hidetsugu Terada** received his Bachelor and Master degrees in Mechanical Engineering from the University of Yamanashi, Japan, in 1986 and 1988, respectively. He then received his Doctorate from the Tokyo Institute of Technology in 1993. Dr. Terada is currently an Associate Professor at the

Graduate School of Medical and Engineering Science at the University of Yamanashi in Kofu, Japan. He serves as the IFToMM Technical Committee member of the “Linkage and cams.” His research interests include gear-less reducers, robotics, and micro-machining.